Available online at www.dergipark.gov.tr

INTERNATIONAL ADVANCED RESEARCHES
and
ENGINEERING JOURNAL

Journal homepage: www.dergipark.gov.tr/iarej

e-ISSN: 2618-575X

International
Open Access

Volume 02
Issue 01

April, 2018

Research Article

Ab-initio calculations of structural, optical and electronic properties of $AgBiS_2$

Seyfettin Ayhan[a] , Gülten Kavak Balcı[a*]

[a] Department of Physics, Dicle University, Diyarbakır, Turkey

ARTICLE INFO

Article history:
Received 05 January 2018
Revised 19 March 2018
Accepted 20 March 2018

Keywords:
$AgBiS_2$
Ab-intio calculations
Wien2k
FPLAPW
Structural properties
Optical properties
Electronic properties

ABSTRACT

In this work, we use first-principles calculations based on density-functional theory generalized gradient approximation (Perdew Burke Ernzerhof, PBE). Cubic and hexagonal $AgBiS_2$ structures have been performed using the self-consistent full-potential linearized augmented plane wave (FPLAPW) method to investigate the structural, optical and electronic properties. We have calculated the ground-state energy, the lattice constant, DOS, band gap and dielectric constant of cubic and hexagonal $AgBiS_2$ by using Wien2k packet. The calculated physical properties of silver bismuth sulfide are compared with the experimental results and good agreement was observed.

1. Introduction

Recently, there are great attention on I–V–VI_2 ternary chalcogenide semiconducting compounds because of their many applications as a solar cell in linear, nonlinear, optoelectronic and thermoelectric devices [1,2,3]. In addition to experimental study there are intensive theoretical study on this material class [4,5]. Silver bismuth sulfide, one of these compounds, (AgBiS2) is a promising candidate for use as novel semiconductors[6, 7].

$AgBiS_2$ is considerable practical concern as a solar cell material, because its energy gap [7,8] is close to the optical energy gap of solar cell absorbers [9].

AgBiS2 has been studied because of exceptional its uncommon electronic and magnetic properties which can be applied in linear, non-linear, optoelectronic, and thermoelectric devices as well as optical recording media [4, 10,11].

$AgBiS_2$ nanocrystals are used in quantum dot-sensitized solar cells and it increases the conversion efficiency [12].

Accurate knowledge of the thermodynamic properties of β-AgBiS2 is very important not only for studies of ore genesis, processing of complex minerals, and the optimization of the extractive metallurgy of the base and precious metals but also for improved manufacturing of novel electronic materials incorporating β-AgBiS2 [4,13].

Ternary silver bismuth sulfide ($AgBiS_2$) is a typical member of I−V−VI_2 family. Bulk AgBiS2 crystallizes in the hexagonal phase (space group, P-3m1) at room temperature,) and transforms to a cubic rocksalt structure (space group, Fm-3m) at around 473 Kelvin[14]. It is known that there exist two phases of $AgBiS_2$, namely, the low temperature phase β-$AgBiS_2$ with a hexagonal structure and the high temperature phase α–$AgBiS_2$ with a cubic structure [10]. It is also some works show that mineral matildite ($AgBiS_2$) have orthorhombic phase with a=8.14 b=7.87 and c=5.69. α-$AgBiS_2$ has face-centered disordered cubic statistically NaCl-type structure with Ag and Bi atoms distributed indistinguishably (0, 0, 0; 0, 1/2,1/2) and S on the

* Corresponding author. Tel.: +90 *0412 2488550-3172*; Fax: +90 *0412 2488300*;
E-mail address: *gulten@dicle.edu.tr*
Note: This study was presented at International Advanced Researches and Engineering Congress 2017 (IAREC'17)

average in the other set of position (1/2, 1/2, 1/2; 0, 0, 1/2) (Figure 1.a.). β–phase of $AgBiS_2$ is hexagonal with space group 139 (P-3m1) and a =4.72, c=19.06 (Figure 1.c) [10,15].

Because of its physical properties, $AgBiS_2$ compound is used at widely area so we aimed to find more information about its physical properties and contribute the literature

In the present study, the ground-state energy, the lattice constant, DOS, band gap, structural, electronic and optical properties of cubic and hexagonal $AgBiS_2$ are investigated. According to our knowledge, no theoretical works have been performed for structural, electronic and optical properties of $AgBiS_2$ using the full-potential linearized augmented plane wave (FPLAPW) method.

This work is organized as follows: Section 2 describes our method and give the computational details, in Section 3 is given to the description of the results and Section 4 is for the conclusions.

2. Computational method

We studied structural, electronic and optical properties of both cubic and hexagonal $AgBiS_2$ compounds with in a self-consistent scheme by solving the Kohn–Sham equations based on Density Functional Theory with generalized gradient approximation (GGA) method [16]. The calculations were performed using the self-consistent full potential linearized augmented plane wave (FPLAPW) method [17] implemented in Wien2k code [18]. We select Perdew-Burke-Ernzerhof Generalized Gradient Approximation (PBE-GGA) exchange and correlation potentials described by Perdew-Burke-Ernzerhof (PBE) [18-21]. In the LAPW method the space is divided into non-overlapping muffin-tin (MT) spheres and interstitial region. We select muffin-tin sphere radii as 2.5 au for Ag and Bi, and 2.08 au for S. The convergence of the basis set was controlled by a cut off parameter $R_{MT}K_{max}$. The $R_{MT}K_{max}$ was selected as 8 value. The magnitude of the largest vector in charge density Fourier expansion (G_{max}) was selected as 12. The separation of valence and core states energy called the cutoff energy was chosen as -7 Ry. During SCF calculation, we select the 0.001e for charge and 0.0001 Ry for energy convergence criteria. For the Brillouin zone (BZ) integration, the tetrahedron method with 159 special k points in the irreducible wedge (2000 k-points in the full BZ) was used to construct the charge density in each self-consistency step.

Structural calculation of hexagonal $AgBiS_2$ was started with experimental lattice constant (a= 4.07, c =19.06 A^0) and atomic coordinate, given in Table 1 [16], and searched for minimum energy depend on volume. The electronic and optical calculations were performed with optimized structure data.

Because of cubic $AgBiS_2$ is disordered and Bi and Ag atoms distributed indistinguishably (Figure 1.a.) the cubic $AgBiS_2$ was studied as supercell 2x2x2. So Ag and Bi were settled in regular order position in NaCl type structure. The produced cell dimensions is 2 times and volume is 8 times larger than disordered unit cell structure (Figure 1.b.).

Table 1. Atomic positions of hexagonal $AgBiS_2$

Atom	x	y	z
Ag1	0	0	0
Ag2	1/3	2/3	0.672
Bi1	0	0	0.5
Bi2	1/3	2/3	0.163
S1	0	0	0.253
S2	1/3	2/3	0.926
S3	1/3	2/3	0.406

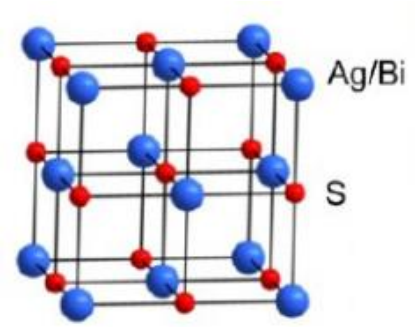

(a)

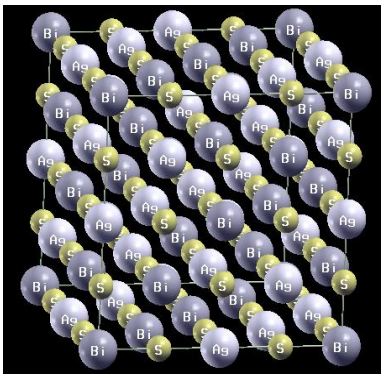

(b)

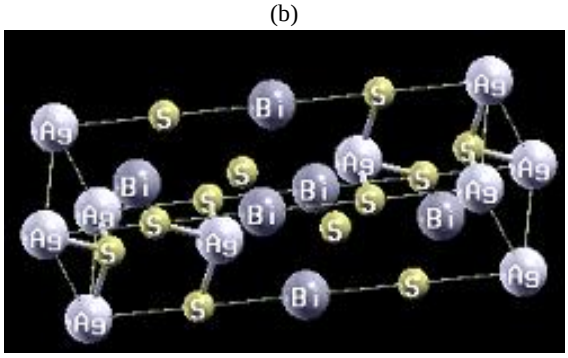

(c)

Figure 1. Unit cell of $AgBiS_2$ (a) NaCl disordered cubic structure, (b) $Ag_{0.5}Bi_{0.5}S$ supercell structure, (c) hexagonal $AgBiS_2$ structure

The volume optimization of supercell performed with ground state energy minimization. The electronic and optical calculations were performed with optimized lattice constant.

3. Results and discussion

3.1. Structural properties

To find ground state energy the total energy was calculated for different volume. The calculated total energies as a function of volume are fitted with Murnaghan's equation of state [22] to determine the ground state properties. We plotted total energy as a function of volume for hexagonal $AgBiS_2$ in Figure 2 and for cubic $Ag_{0.5}Bi_{0.5}S$ in Figure 3.

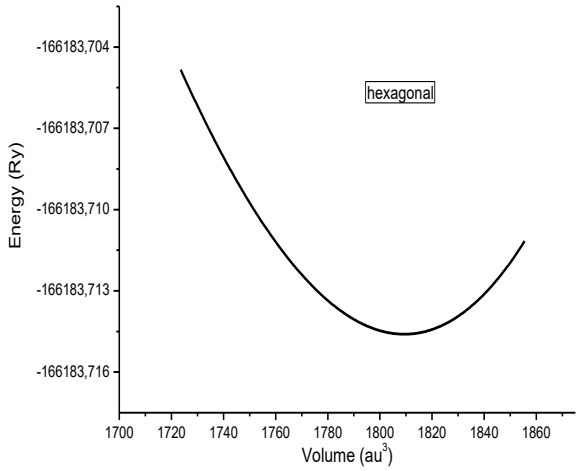

Figure 2. Dependence of total energy on unit cell volume for hexagonal AgBiS2

In Figure 2, it is can be seen that the minimum value of energy corresponds to the ground state volume 1809,3644 au^3 . Therefore, the calculated lattice constants for hexagonal $AgBiS_2$ are found a= 4,02 A^0 and c=19,054 A^0. Meanwhile, the experimental values of lattice constants are:

a= 4.07 A^0, c =19.06 A^0 [15]

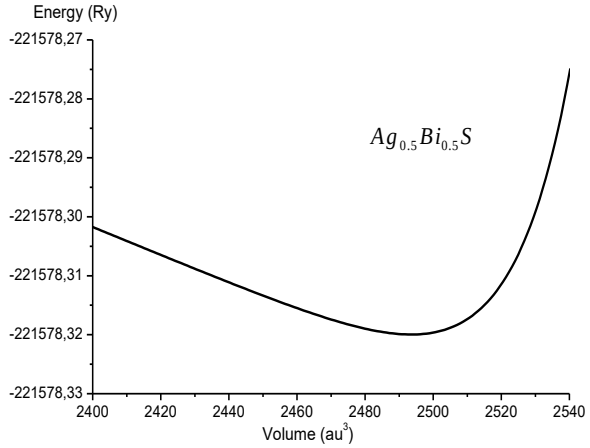

Figure 3. Dependence of total energy on unit cell volume for cubic $AgBiS_2$

In Figure 3, it is seen that the minimum value of energy corresponds to the ground state volume 2493,5740 au^3 Therefore, the calculated lattice constant for cubic $Ag_{0.5}Bi_{0.5}S$ is found a=11.3910 A^0. Meanwhile, the experimental value of lattice constant a = 5.648 A^0. The calculated results are good agreement with experimental data if we consider supercell is 2 times larger than experimental unit cell.

Calculated volume cell dimensions, bulk modulus (B) and minimum energy (E) values for both phase are given in Table 2

Table 2. Calculated cell dimensions, bulk modulus and minimum energy of cubic and hexagonal $AgBiS_2$ compound

Parameter	a (A^0)	c (A^0)	B (GPa)	E (Ry)
Hexagonal $AgBiS_2$	4,068	19,054	80,07	-166183,71460
Cubic $Ag_{0.5}Bi_{0.5}S$	11,391	-	54,8389	-221578,31996

The structural stability of cell is determined by cohesive energy calculation. According to cohesive energy [23]:

$$E_{coh} = -\frac{E^{tot}_{AgBiS_2} - kE^{tot}_{Ag} - mE^{tot}_{Bi} - nE^{tot}_{S}}{k+m+n}$$

Where $E^{tot}_{AgBiS_2}$, E^{tot}_{Ag}, E^{tot}_{Bi}, E^{tot}_{S} are total energy for $AgBiS_2$ unit cell, isolated Ag, Bi and S atom, respectively. k, m and n indexes refer to the number of each atom in the unit cell.

We obtained the value of cohesive energy 2.38 eV/atom for cubic $Ag_{0.5}Bi_{0.5}S$ and 2.33 eV/atom for hexagonal phase $AgBiS_2$.

3.2. Electronic properties

It is well known that the electronic band structure and density of states (DOS) are important quantities to determine the crystal structure [24]. In order to understand bonding character clearly, the density of states (DOS) is calculated, as shown in Figure 4 and Figure 5. In the figures, Fermi level were settled at zero point. Evidently, the total DOS's of the two phases exhibit semiconductor feature. It can be seen from Figure 4.b and 5.b that the big DOS contribution at the valence band are given by silver. At the conducting band, the contribution of silver decreases and the contribution of bismuth increases. So we can say that charge transfer is occurred from silver to bismuth at Fermi energy level, and the bond character of both phase are largely covalent bonding.

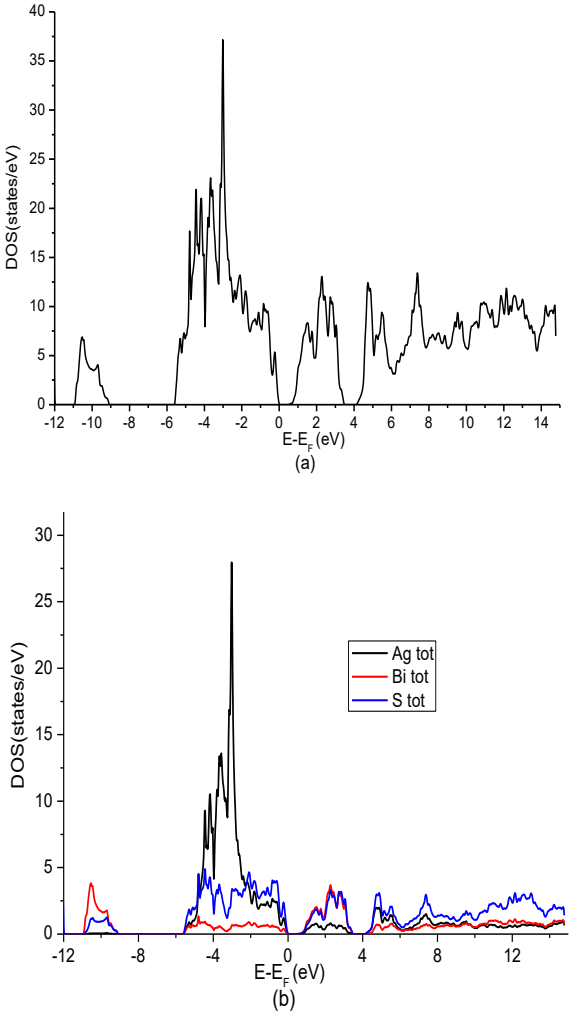

Figure 4. Calculated total and partial DOS for hexagonal $AgBiS_2$ (a) total DOS (b) partial DOS

We plotted an electronic band chart to understand the electronic properties of the both cubic and hexagonal phase structures (Figure 6. and Figure 7.). At the figures the Fermi energy level set to origin. In the Figure 6, top of valence band is located between the high symmetry points K and Γ while the bottom of conduction band is located at the A in the Brillion Zone [25]. Therefore, hexagonal $AgBiS_2$ has an indirect band gap with value of 0.463 eV.

In the Figure 7, top of valence band is located at the high symmetry point X while the bottom of conduction band is located at the L in the BZ. Therefore, cubic $AgBiS_2$ has an indirect band gap with value of 0.83 eV. The calculated band structure is in good agreement with previous works [14].

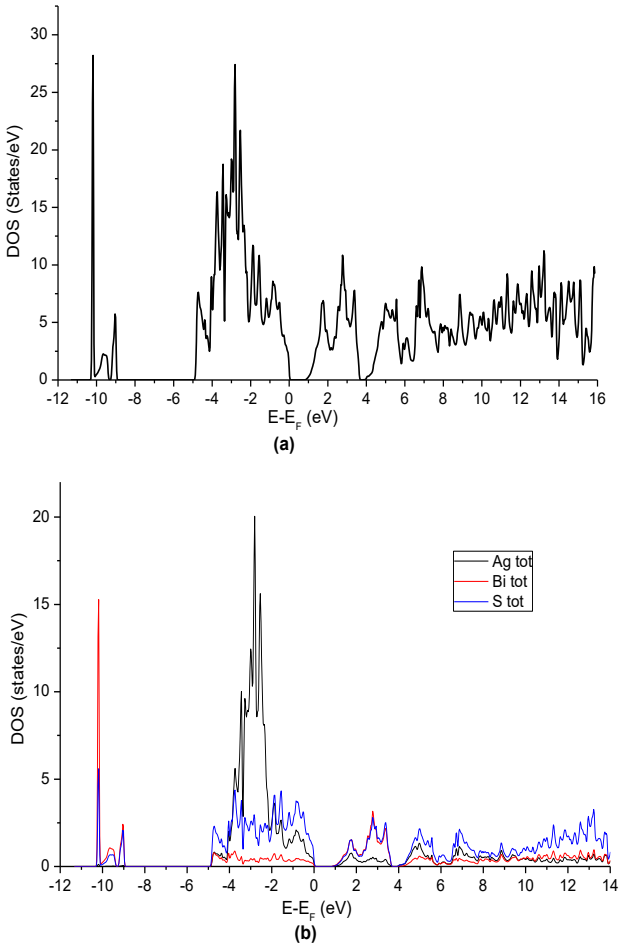

Figure 5. Calculated total and partial DOS for cubic $AgBiS_2$ (a) total DOS (b) partial DOS

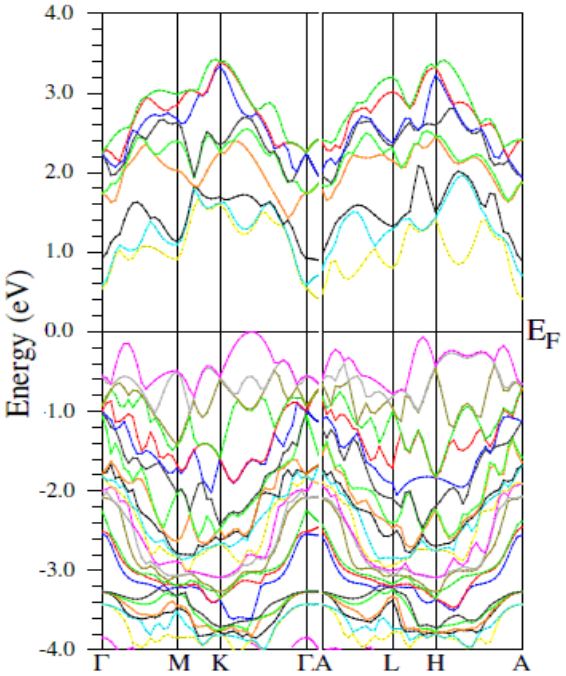

Figure 6. Electronic band plot of hexagonal $AgBiS_2$

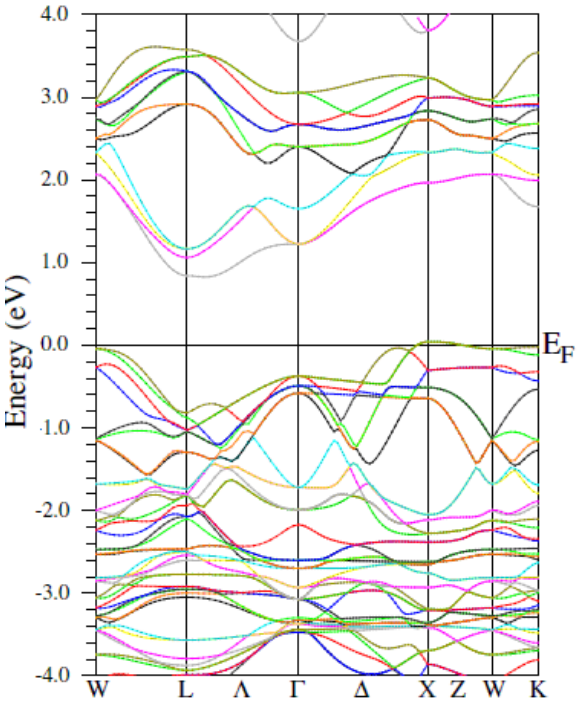

Figure 7. Electronic band plot of cubic $AgBiS_2$

3.3. Optical properties

Determining optical properties of materials let us to develop new optoelectronic applications. So we calculated dielectric function, optical conductivity, absorption, energy loss function and reflection of both cubic and hexagonal $AgBiS_2$ to contribute this area. All calculations performed with no intra band contributions added.

3.3.1. Dielectric function

The calculation of complex dielectric function can be considered as one of the best approaches to investigate the optical properties of materials [26]. The optical response of a medium at all photon energies is described by the dielectric function:

$$\varepsilon(\omega) = \varepsilon_1(\omega) + i\varepsilon_2(\omega)$$

The real part $\varepsilon_1(\omega)$ and the imaginary part $\varepsilon_2(\omega)$ corresponds to the dispersive and absorptive behavior of the material, respectively. The real and imaginary parts of dielectric function of cubic and hexagonal phase of $AgBiS_2$ calculated without the addition of spin orbit interaction are plotted in Figure 8 and Figure 9.

As seen in the Figure 8 and 9, the static values of real part of dielectric constant, ε_0, is 20 and 16.4, respectively.

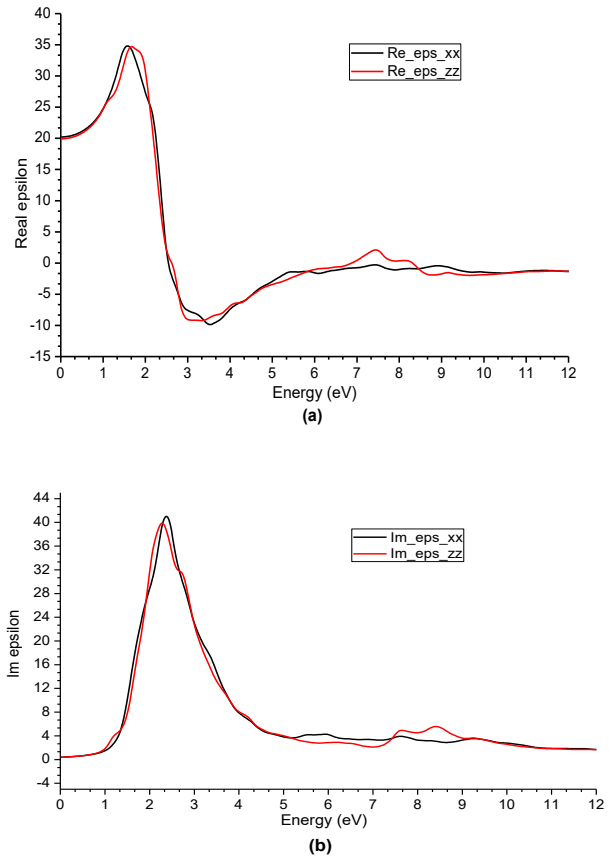

Figure 8. Calculated real and imaginary part of epsilon hexagonal $AgBiS_2$ a) real part epsilon (b) imaginary part epsilon

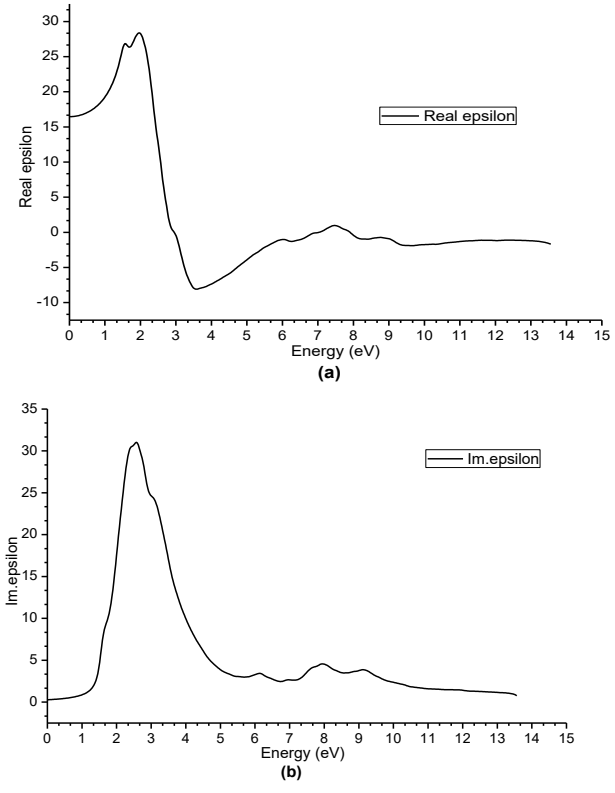

Figure 9. Calculated real and imaginary part of epsilon cubic phase of $AgBiS_2$ a) real part b) imaginary part

3.3.2. Absorption coefficient

The absorption coefficient determines the ability of material to absorb the incident photon of specific frequency [25]. We can write the absorption coefficient:

$$\alpha(\omega)_j = 2\omega / c(-\mathrm{Re}(\varepsilon(\omega)_j) + \left|\varepsilon(\omega)_j\right| / 2)^{1/2}$$

Calculated absorption coefficient of $AgBiS_2$ are plotted in Figure 10.

It can be seen from Figure 10, **t**he absorption part of hexagonal $AgBiS_2$ spectra starts with 0.8 eV energy, and the absorption part of cubic $AgBiS_2$ spectra starts with nearly 1 eV energy.

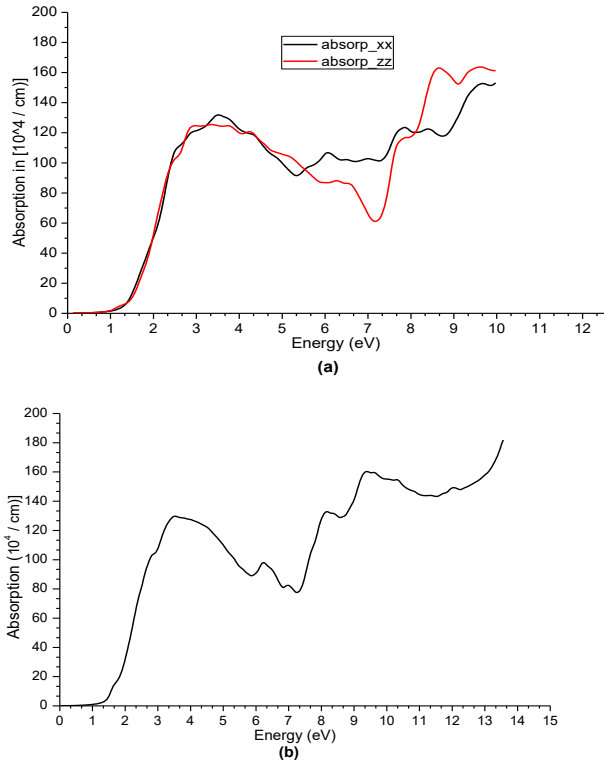

Figure 10. Calculated optical absorption of $AgBiS_2$
a) hexagonal phase b) cubic phase

3.3.3. Optical conductivity

The optical conductivity $\sigma(\omega) = \alpha nc / 4\pi$ corresponds to the conduction of electrons produced when photon of certain frequency is incident upon a material [25]. The optical conductivity of hexagonal $AgBiS_2$ given in Figure 11.a. E_0 =0.65 eV and the first peak appears for xx direction 2.408 eV and for zz direction 2.327 eV. The optical conductivity(sigma) has the maximum value of xx direction 13227 [1 / (Ohm cm)] and 12381 [1 / (Ohm cm)] for zz direction corresponds to visible region of the electromagnetic spectrum.

The optical conductivity of cubic $AgBiS_2$ shown in Figure 11.b. E_0 =0.8 eV, the first peak appears for 3.088 eV and the optical conductivity has the maximum value of 10064 [1 / (Ohm cm)] corresponds to visible region of the electromagnetic spectrum.

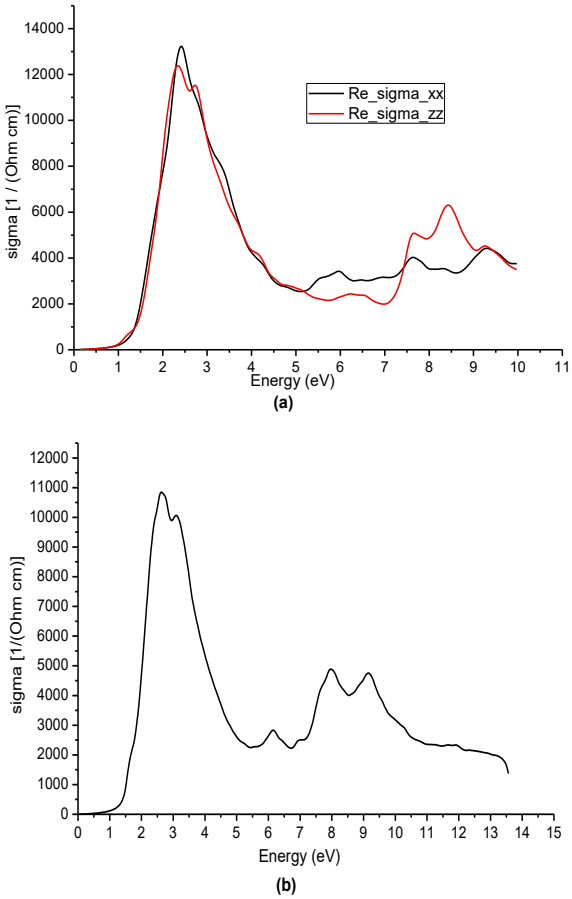

Figure 11. Calculated optical conductivity of AgBiS2
a) hexagonal phase, b) cubic phase

3.3.4. Reflectivity

The value of reflectivity at the zero frequency is described as the static reflectivity (R_0). For the cubic phase of $AgBiS_2$, R_0 =0.36 and for the hexagonal $AgBiS_2$ R_0 =0.4 (Figure 12.a.). It can be seen from figure the reflectivity has many peaks depending on energy. The reflectivity has a maximum value R_{max}=0.617 at the 4.14 eV energy and minimum value R_{min} = 0.186 at 7.31 eV energy for cubic $AgBiS_2$.

The maximum reflectivity values of hexagonal $AgBiS_2$ are 0.656 at the 3.36 eV energy for xx direction and 0.638 at the 2,48 eV energy for zz direction. The minimum values of reflectivity for hexagonal phase are 0.281 at the 7.39 eV energy at xx direction and 0.133 at the 7.17 eV energy for zz direction.

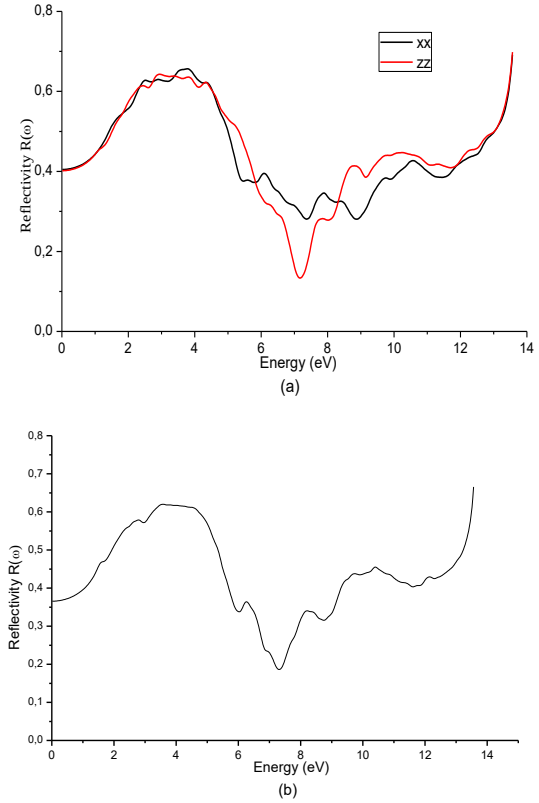

Figure 12. Calculated reflectivity coefficient, R(ω) index a) hexagonal phase $AgBiS_2$ b) cubic phase $AgBiS_2$

3.3.5. Energy loss function

The energy loss function L(ω) describes the frequencies correspond to the plasma resonance. Plasma resonance occurs when the frequency of incident radiations matches with the frequency of plasmas. The energy loss function depend on incident energy for cubic and hexagonal of $AgBiS_2$ is plotted in Figure 13. The loss function shows peaks at 5.37 eV, 7.22 eV, 8.72 eV and 11.44 eV for xx direction and at 6.93 eV, 7.96 eV, 9.13 eV, 9.83 eV, 11.68 eV for zz direction(Figure 13.a.), and for cubic phase shows peaks at 5.89 eV, 6.79 eV, 8.67 eV and 12.31 eV(Figure 13b).

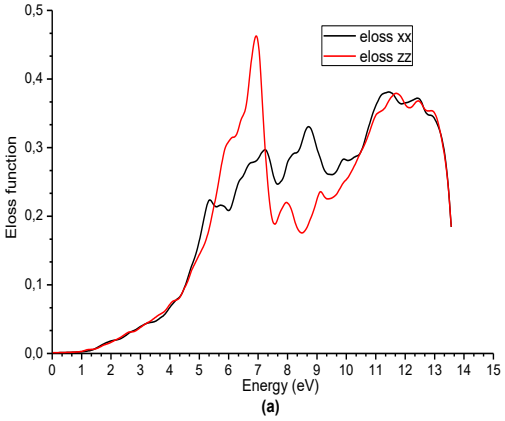

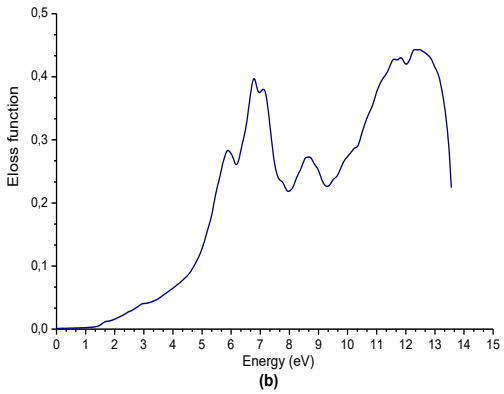

Figure 13. Calculated electron energy loss spectrum of $AgBiS_2$ a) hexagonal phase b) cubic phase

4. Conclusions

We have investigated structural, electronic and optical properties both cubic and hexagonal $AgBiS_2$ using all electrons full potential linearized augmented plane wave (FPLAPW) method based on DFT within generalize gradient approximation (GGA). We calculated ground state energy, cell constants, bulk modulus, and cohesive energy. The calculated cell constants are good agreement with experimental works. Calculated cohesive energy of compounds show that the structures have mechanical stability.

DOS calculation of both phase of cubic and hexagonal are plotted. DOS plot show the both phase have semiconducting features. The DOS plots show that the bond character of compounds are covalent bonding. The calculated electronic band structure shows that the both phase of $AgBiS_2$ are indirect band gap semiconductor. The calculated band gap of cubic phase is 0.83 eV and it has a good agreement with compare to other experimental results (bulk 0.8 eV, monocrystalline 1 eV) [14]. The hexagonal $AgBiS_2$ has indirect band gap with 0,463 eV.

To determine optical properties of $AgBiS_2$ we calculated optical parameters such as dielectric function, absorption coefficient, refractive index, reflectivity and energy loss function for radiation up to 14.0 eV.

Calculated electronic and optical properties of $AgBiS_2$ show that the both phase of $AgBiS_2$ compounds are good candidate for electronic devices, optical devices and solar cell applications.

Acknowledgement

This research was supported by the Dicle University Scientific Research project coordination unit (project no: FEN.15.016). Thanks to Prof. Peter Blaha and Prof. Karlheinz Schwarz for supplied free Wien2k code to us.

References

1. Samanta, L.K., S. Chatterjee, On the linear, nonlinear, and optoelectronic properties of some multinary compound semiconductors, Phys. Status Solidi B, 1994, 182, K85.

2. Aliev, S.A., S.S. Raginov, Thermoelectric Proper- ties of Ag–Sb–Te Materials, Neorg. Mater, 1992, 28- 329.

3. Saadi B. , D. Maouche, N. Bouarissa, Y. Medkour, First principles study of structural, electronic and optical properties of AgSbS2,Materials Science in Semiconductor Processing,16, 2013, 1439–1446

4. Tesfaye, F., Taskinen, P., Electrochemical study of the thermodynamic properties of matildite (β-$AgBiS_2$) in different temperature and compositional ranges, Solid State Electrochem, 2014, 18:1683–1694

5. Hoang, K., S.M. Mahant, Atomic and electronic structures of I-V-VI_2 ternary chalcogenides, Journal of Science: Advanced Materials and Devices Volume 1, Issue 1, March 2016, 51-56

6. Shen, G., D. Chen, K. Tang, Y. Qian, Polyol mediated synthesis of nanocrystalline M_3SbS_3 (M = Ag, Cu), J. Cryst. Growth 252, 2003, 199.

7. Nakamura, M., H. Nakamura, T. Ohsawa, M. Imura, K. Shimamura, N. Ohashi, AgBiS2 single crystal grown using slow cooling method and its characterization, Journal of Crystal Growth, 2015, 411, 1-3.

8. Pejova, B., D. Nesheva, Z. Aneva, A. Petrova, Photoconductivity and Relaxation Dynamics in Sonochemically Synthesized Assemblies of $AgBiS_2$ Quantum Dots, J. Phys. Chem., 2011, C 115, 37.

9. Zdanowicza, T., T. Rodziewiczb, M. Zabkowska-Waclawek, Theoretical analysis of the optimum energy band gap of semiconductors for fabrication of solar cells for applications in higher latitudes locations,Sol. Energy Mater. Sol. Cells ,2005, 87, 757-769.

10. Chen, D., G.Z. Shen, K.B. Tang, X. Jiang, L.Y. Huang, Y. Jin, Y.T. Qian, Microwave synthesis of $AgBiS_2$ dendrites in aqueous solution, Inorg. Chem. Commun., 2003, 6, 710–712.

11. Yan, J., J. Yu, W. Zhang, Y. Li, X. Yang, A. Li, X. Yang, W. Wang, J. Wang, Synthesis of Cu_3BiS_3 and AgBiS2 crystallites with controlled morphology using hypocrellin template and their catalytic role in the polymerization of alkyls lane, J. Mater. Sci. 2012, 47 4159–4166.

12. Liang, N., W. Chen, F. Dai, X. Wu,W. Zhang, Z. Li, J. Shen, S. Huang, Q. He, J. Zai, N. Fang and X. Qian, Homogenously hexagonal prismatic AgBiS2 nanocrystals: Controlled synthesis and application in quantum dot-sensitized solar cells. CrystEngComm, 2015, 17, 1902-1905.

13. Huang, P. C., Yang, W. C., and Lee, M. W., $AgBiS_2$ Semiconductor-Sensitized Solar Cells, *J. Phys. Chem. C*, 2013, 117 (36), pp 18308–18314.

14. Satya N. G. and K. Biswas, Cation Disorder and Bond Anharmonicity Optimize the Thermoelectric Properties in Kinetically Stabilized Rocksalt $AgBiS_2$ Nanocrystals, Chem. Mater., 2013, 25, 3225−3231.

15. Galler, S. and J.H., Wernick Ternary semiconducting compounds with sodium chloride-like structure: $AgSbSe_2$, $AgSbTe_2$, $AgBiS_2$, $AgBiSe_2$ acta crystallographica, 1959,12, 46-54.

16. Perdew, J.P., J.A. Chevary, S.H. Vosko, K.A. Jackson, M.R. Pederson, D.J. Singh, C.Fiolhais, Atoms, molecules, solids, and surfaces: Applications of the generalized gradient approximation for exchange and correlation, Phys. Rev. B., 1992, 46, 6671.

17. Singh, D.J., Planes Waves, Pseudo-Potentials and the LAPW Method, Kluwer Academic Publishers, 1994, .Boston, Dortrecht, London.

18. Blaha, P., K. Schwarz, G.K.H. Madsen, D. Kvasnicka, J. Luitz, WIEN2k, An Augmented Plane Wave + Local Orbitals Program for Calculating Crystal Properties, Karlheinz Schwarz, Techn Universitat Wien, Austria, 2001, ISBN:3-9501031-1-2.

19. Perdew, J.P., K. Burke, Y. Wang, Physical Review, Erratum: Generalized gradient approximation for the exchange-correlation hole of a many-electron system, Phys. Rev. 1996, B 54, 16533.

20. Perdew, J.P., S. Burke, M. Ernzerhof, Generalized Gradient Approximation Made Simple, Physical Review Letters, 1996, 773865.

21. Kervan, N. S. Kervan, A first-principle study of half-metallic ferrimagnetism in the Ti_2CoGa Heusler compound, Journal of Magnetism and Magnetic Materials, 2012, 324, 4, 645-648.

22. Murnaghan, F.D., Proceedings of the National Academy of Sciences of the United States of America, 1947, 30, 244.

23. Mosayeb N., J. Jalilian, A.H. Reshak, Electronic and optical properties of pentagonal-B_2C monolayer: A first-principlescalculation, Int. J. Mod. Phys. B, 2017, **31**, 1750044.

24. Erdinc, B., M.N. Secuk, M. Aycibin, S.E. Gülebagan, E. K. Dogan, H. Akkus, Ab-initio Calculations of Structural, Electronic, Optical, Dynamic and Thermodynamic Properties of HgTe and HgSe, Computational Condensed Matter, 4, 2015, 6-12.

25. Setyawan, W., S. Curtarolo, High-throughput electronic band structure calculations: Challenges and tools, Computational Materials Science, 2010, 49, 299–312.

26. Hilal, M., R. Bahroz, S.H. Khan, A. Khan, Investigation of electro-optical properties of InSb under the influence of spin-orbit interaction at room temperature, Materials Chemistry and Physics, 2016, 184, 41-48.